

Radiobiologic Principles in Radionuclide Therapy

Amin I. Kassis, PhD; and S. James Adelstein, MD, PhD

Department of Radiology, Harvard Medical School, Boston, Massachusetts

Although the general radiobiologic principles underlying external beam therapy and radionuclide therapy are the same, there are significant differences in the radiobiologic effects observed in mammalian cells. External beam and brachytherapy emissions are composed of photons, whereas radiations of interest in radionuclide therapy are particulate. The special features that characterize the biologic effects consequent to the traversal of charged particles through mammalian cells are explored with respect to DNA lesions and cellular responses. Information about the ways in which these radionuclides are used to treat cancers in experimental models are highlighted.

Key Words: α -particle emitters; Auger-electron emitters; β -particle emitters; radiobiology; radionuclide therapy

J Nucl Med 2005; 46:4S-12S

Although the general radiobiologic principles underlying external beam therapy and radionuclide therapy are the same, there are significant differences in the radiobiologic effects observed in mammalian cells (1). External beam and brachytherapy emissions are composed of photons, whereas radiations of interest in radionuclide therapy are particulate. Moreover, targeted radionuclide therapy is characterized by (a) extended exposures and, usually, declining dose rates; (b) nonuniformities in the distribution of radioactivity and, thus, absorbed dose; and (c) particles of varying ionization density and, hence, quality.

This introductory article emphasizes the special features that characterize biologic effects consequent to the traversal of charged particles through mammalian cells and looks at what has been learned from the use of these radionuclides in treating cancers in experimental models.

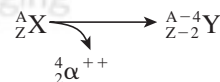
PARTICULATE RADIATION

Energetic Particles

In general, the distribution of diagnostic and therapeutic radiopharmaceuticals throughout a targeted solid tumor is nonhomogeneous. This is mainly the result of the inability of the radiolabeled molecules to evenly penetrate dissimilar

regions within a solid tumor mass or differences in specific binding-site densities of individual tumor cells. For imaging purposes, the consequence of these nonuniformities is nominal (the distribution of radioactive emissions appears uniform at the organ/tissue level). With radiopharmaceuticals labeled with energetic α - and β -particle emitters (range of emitted particle greater than the diameter of the targeted cell), however, such nonuniformity will lead to dosimetric nonhomogeneities (i.e., major differences in absorbed doses to individual tumor cells). Consequently, the mean absorbed dose is not a good predictor of radiotherapeutic efficacy.

α -Particle Emitters. Over the past 30 y, the therapeutic potential of several α -particle-emitting radionuclides has been assessed. These particles are positively charged with a mass and charge equal to the helium nucleus, and their emission leads to a daughter nucleus with 2 fewer protons and 2 fewer neutrons:



These particles have energies ranging from 5–9 MeV with corresponding tissue ranges of 5–10 cell diameters, travel in straight lines, and deposit 80–100 keV/ μ m along most of their track (rate of energy deposition increases to \sim 300 keV/ μ m toward the end of the track) (Table 1). Consequently, in the case of cell self-irradiation, the following 2 factors must be considered when evaluating the therapeutic efficacy of α -particle emitters: (a) distance of the decaying atom from the targeted mammalian cell nucleus as it relates to the probability of a nuclear traversal (Fig. 1); and (b) contribution of heavy ion recoil of the daughter atom when the α -particle emitter is covalently bound to nuclear DNA (2). Of equal importance is the magnitude of cross-dose (from radioactive sources associated with one cell to an adjacent/nearby cell), because this will vary considerably, depending on the size of the labeled cell cluster and the fraction of cells labeled (3).

β -Particle Emitters. Current radionuclide therapy in humans is based almost exclusively on energetic β -particle-emitting isotopes. β -particles are negatively charged electrons that are emitted from the nucleus of a decaying radioactive atom (1 electron/decay) and that have various energies (zero up to a maximum) and, thus, a distribution of

Received Apr. 21, 2004; revision accepted Aug. 16, 2004.
For correspondence or reprints contact: Amin I. Kassis, PhD, Department of Radiology, Harvard Medical School, 200 Longwood Ave., Armenise Building, Boston, MA 02115.
E-mail: amin_kassis@hms.harvard.edu

TABLE 1
General Characteristics of Therapeutic Radionuclides

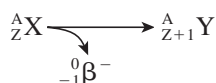
Decay	Particles	$E_{(min)}-E_{(max)}$	Range	LET
β^- -particle	Energetic electrons	50–2,300 keV*	0.05–12 mm	0.2 keV/ μm
α^{++} -particle	He nuclei	5–9 MeV†	40–100 μm	80 keV/ μm
EC/IC	Nonenergetic electrons	eV–keV†	2–500 nm	4–26 keV/ μm

*Average (>1% intensity); continuous distribution of energy.

†Monoenergetic.

EC = electron capture; IC = internal conversion.

ranges (Table 1). After emission, the daughter nucleus has 1 more proton and 1 less neutron.



As these β -particles traverse matter, they lose kinetic energy and eventually follow a contorted path and come to a stop. Because of their small mass, the recoil energy of the daughter nucleus is negligible. In addition, the linear energy transfer (LET) of these energetic, light, and negatively charged (-1) particles is very low (~ 0.2 keV/ μm) along their up-to-a-centimeter path (i.e., they are sparsely ionizing), except for the few nanometers at the end of the range (Fig. 2). Consequently, their use as therapeutic agents necessitates the presence of high radionuclide concentrations within the targeted tissue. An important implication of the long range of each emitted electron is the production of cross-fire, a circumstance that negates the need to target every cell within the tumor. As with α -particles, the prob-

ability of the emitted β -particle traversing the targeted cell nucleus depends to a large degree on the distance of the decaying atom from the cell nucleus and the radius of the latter (Fig. 1). Finally, many of the β -particle-emitting radionuclides used for therapy also release γ -photons that generally do not add significantly to the dose delivered to the target tissue.

Nonenergetic Particles

During the decay of certain radioactive atoms, a vacancy is formed (most commonly in the K shell) as a consequence of electron capture (EC) or internal conversion (IC).

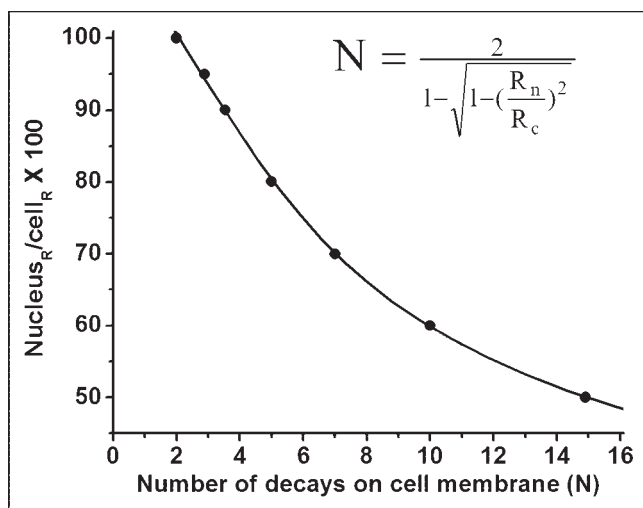
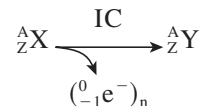
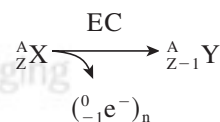


FIGURE 1. Number of radioactive atoms needed to assure traversal of cell nucleus by a single energetic particle as function of distance from nuclear membrane. Nuclear-to-cell radius (percentage) plotted as function of number of decays in cell membrane.

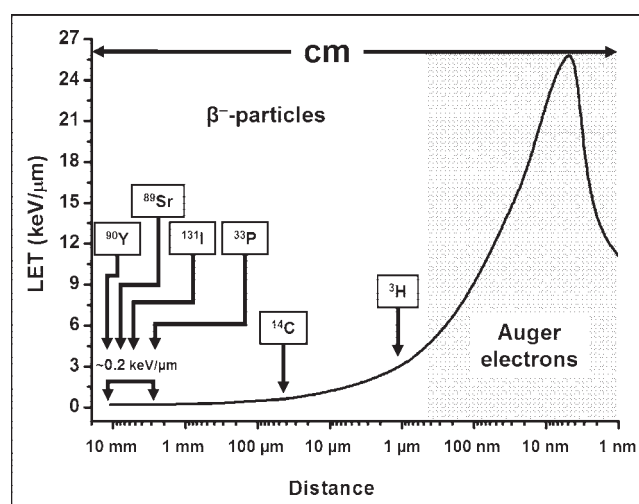


FIGURE 2. Rate of energy loss of electrons as function of traversed distance.

Such vacancies are rapidly filled by electrons dropping in from higher shells. This process leads to a cascade of atomic electron transitions that move the vacancy toward the outermost shell. Each inner-shell electron transition results in the emission of a characteristic X-ray photon or an Auger, Coster–Kronig, or super Coster–Kronig monoenergetic electron (collectively called Auger electrons). An atom undergoing EC or IC emits, on average, 5–30 Auger electrons with energies ranging from a few eV to approximately 1 keV (Table 1). In addition to the shower of low-energy electrons, this form of decay leaves the daughter atom with a high positive charge, resulting in subsequent charge-transfer processes. The very low energies of Auger electrons have 2 major consequences. First, these light, negatively charged (-1) particles travel in contorted paths, and their range in water is from a fraction of a nanometer up to ~ 0.5 μm (Table 1). Second, multiple ionizations (4–26 keV/ μm) occur in the immediate vicinity (within a few nanometers) of the decay site (Fig. 2), reminiscent of ionizations observed along the path of an α -particle (4–6). The short range of Auger electrons also necessitates their close proximity to the radiosensitive target (DNA) for radiotherapeutic effectiveness. This is because of the precipitous drop in energy density as a function of distance in nanometers (7,8).

RADIOBIOLOGY

Molecular Lesions

There is general agreement that the principal target for the biologic effects of ionizing radiation is DNA. Several different lesions are produced (e.g., single-strand breaks, double-strand breaks [DSB], base damage, DNA–protein cross-links, and multiply damaged sites [MDS]). In general, these lesions are repaired with high fidelity, the exceptions being DSB and MDS. These lesions may be produced by direct ionization of DNA (direct effect) or by the interaction of free radicals (mostly hydroxyl radicals produced in water molecules that diffuse a few nanometers) with DNA, an interaction that may be modified by radical scavengers.

The distribution of ionizations within DNA and the type of lesion created depend on the nature of the incident particle and its energy. For α -particles, high ionization densities occur along a linear track (Fig. 3, bottom), whereas for energetic β -particles ionizations along the linear track are infrequent (Fig. 3, top). Low-energy electrons (e.g., Auger electrons) generate clusters of high ionization density along an irregular path (Fig. 3, center). DSB induced by high specific ionization (α -particles and Auger-electron cascades) are less repairable than those created by more sparsely ionizing radiation.

Cellular Responses

Clonal Survival. When mammalian cells are acutely exposed (high dose rate) to low-LET ionizing radiation, their ability to divide indefinitely declines as a function of radiation dose. The shape of the survival curve depends on the

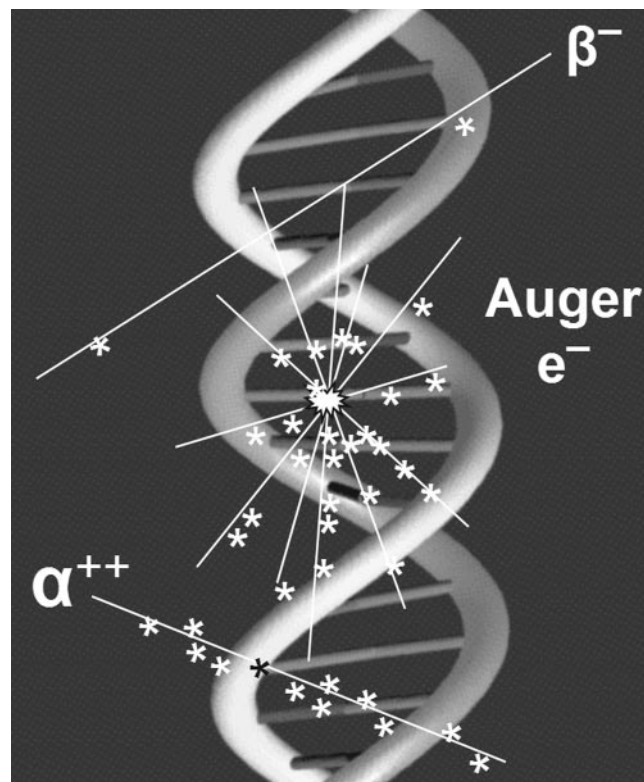


FIGURE 3. Local density of ionizations (*) produced along track (.) of energetic β -particles, Auger electrons, and α -particles.

density of ionizations (Fig. 4). For densely ionizing radiation (α -particles and Auger-electron cascades), the logarithmic response is linear ($-\ln SF = \alpha D$), where SF is the survival fraction and D is the absorbed dose. For sparsely ionizing irradiation (photons and energetic β -particles), the logarithmic response is linear quadratic ($-\ln SF = \alpha D + \beta D^2$). The βD^2 term is thought to represent accumulated and repairable damage. The linear and quadratic contributions to cell killing are equal at the dose (D) that is equal to the ratio of α to β (i.e., when $\alpha D = \beta D^2$ or $[D = \alpha/\beta]$).

Because sparsely ionizing radiation produces repairable sublethal damage, dose–response curves are sensitive to dose rate, with lower dose rates being less damaging than higher ones. In radionuclide therapy this is particularly important when the physical half-life of the tagging isotope is close to the effective half-life. As with fractionated external beam therapy, the total dose from continuous low-dose radionuclide therapy is less effective than a single dose of the same magnitude (i.e., for a comparable biologic effect, a larger dose is required) (9).

Division Delay and Programmed Cell Death. After irradiation, delay in the progression of dividing cells through their cell cycle is a well documented phenomenon. It is reversible, and its length is dose dependent. It occurs only at specific points in the cell cycle and is similar for both surviving and nonsurviving cells. Cells in premitotic G2 of the cell cycle show maximum delay, cells in G1 have little

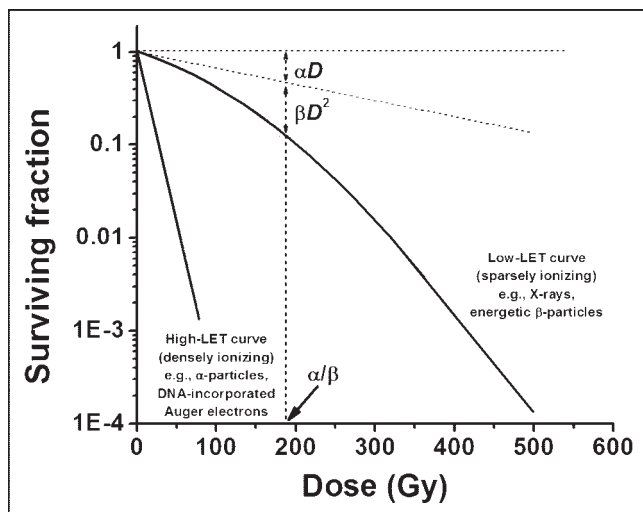


FIGURE 4. Survival of mammalian cells after high- or low-LET irradiation.

delay, and those in S have a moderate delay, whereas cells in mitosis continue through division basically undisturbed. As a result, upon irradiation many cells accumulate at the G2/M boundary, thus altering the mitotic index. Because all phases of the cell cycle are not equally radiation sensitive, these changes in mitotic index may also result in changes to the dose–response curve. Breakthroughs after division delay, as occur at low dose rates, allow cells to proceed through the cell cycle and, if not sterilized, to repopulate tumors or normal tissues.

Division delay also allows irradiated cells time to determine their fate. When cells are irradiated and DNA is damaged, the damage is sensed and various genes are activated. Cells are held at checkpoints (usually G2/M but occasionally G1/S), awaiting repair of DNA, and then proceed through the cell cycle. Alternatively, damage may be nonreparable, and the cells are induced to undergo programmed cell death or apoptosis. The apoptotic pathways are under tight genetic regulation, with the tumor suppressor gene *p53* playing a central role. Cellular responses are variable and require the action of certain proteolytic caspases. Lymphoid tumor cells are more likely to undergo apoptosis than epithelial cells, which may explain the success of radioimmunotherapy in certain lymphomas. In epithelial cells, apoptosis appears to account for only a small portion of clonal cell death.

Oxygen Enhancement Ratios. Oxygen radiosensitizes mammalian cells to the damaging effects of radiation. Hypoxic cells can be as much as 3-fold more radioresistant than well-oxygenated cells. It is believed that after irradiation, oxygen enhances free radical formation or blocks reversible and repairable chemical alterations. The oxygen effect is highest for low-ionization-density radiation (high-energy β -particles) and quite low for high-LET radiation (α -particles and low-energy electrons, including Auger-electron

cascades). In the former instance, the presence of hypoxic regions within tumors is believed to be a major cause of radiotherapeutic failure.

Bystander Effect. The term “bystander effect” is applied to the biologic responses of cells that neighbor irradiated cells but have not been irradiated themselves. Increased mutation rates and decreased survival rates have been reported. Originally observed with external α -particle beams in vitro, the phenomenon has been observed with intranuclear ^{125}I decay in cancer cells growing subcutaneously in vivo (Fig. 5). These observations have negated a central tenet of radiobiology: that damage to cells is caused only by direct ionization or by free radicals generated as a consequence of the deposition of energy within the nuclei of mammalian cells. The importance of the bystander effect as an enhancer of radiotherapeutic efficacy is yet to be determined.

Self-Dose, Cross-Fire, and Nonuniform Dose Distribution. At the tissue level, when radionuclides are used for therapy, cells may be irradiated by decays taking place on or within themselves (self-dose) or in distant or neighboring cells (cross-fire). Because of geometric factors associated with linear paths, the self-dose from energetic α - and β -particles is quite dependent on their position on or within the tumor cell (Fig. 1), whereas that for Auger-electron emitters depends on the proximity of the decaying atom to DNA.

In targeted radionuclide therapy, the distribution of radioactivity and, hence, absorbed doses, tend to be nonuniform. Consequently, higher doses are required to sterilize the targeted cells. Mathematic modeling has led Humm et al. (10) to predict that the difference in the doses needed for a similar

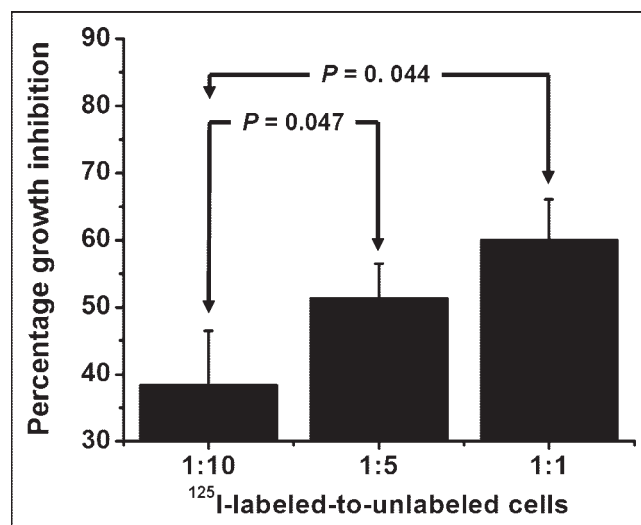
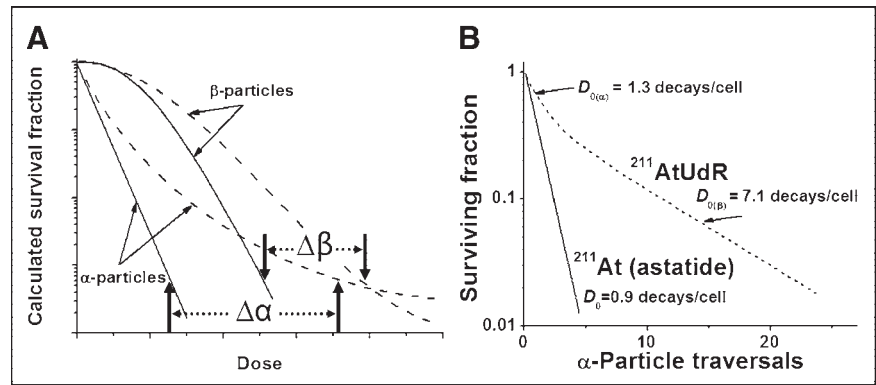


FIGURE 5. Bystander effect observed in vivo in mouse adenocarcinoma model. Human colon LS174T adenocarcinoma cells were prelabeled with lethal doses of DNA-incorporated ^{125}I -UdR, mixed with unlabeled cells at ratios indicated, and injected subcutaneously in mice. Bystander effect is indicated by percentage growth inhibition in vivo of unlabeled cells.

FIGURE 6. (A) Schematic representation of mammalian-cell survival curves after uniform irradiation with α - and β -particles (solid lines) and departure from exponential decrease when radionuclides are not uniformly distributed (broken lines) (10). (B) Survival of mammalian cells exposed in suspension to ^{211}At -astatide or ^{211}At -UdR (only 50% of cells labeled) (2,14).



decrease in survival fraction between uniform and nonuniform dose distribution of α -particle-emitting radionuclides is greater ($\Delta\alpha > \Delta\beta$) than that for energetic β -particles (Fig. 6A). A mathematic model that examines the impact of dose non-uniformity and dose-rate effect on therapeutic response has been described (Fig. 7) (11). From this model, one would predict that as the absorbed dose distribution becomes less uniform, the surviving fraction would increase for any mean absorbed dose; that a nonuniform dose distribution would become proportionately less effective as the absorbed dose increases; and that the difference in survival fraction resulting from uniform versus nonuniform doses would become more pronounced as the radiosensitivity of tumor cells increases.

EXPERIMENTAL THERAPEUTICS

Energetic Particles

α -Particle Emitters. The application of α -particle-emitting radionuclides as targeted therapeutic agents continues

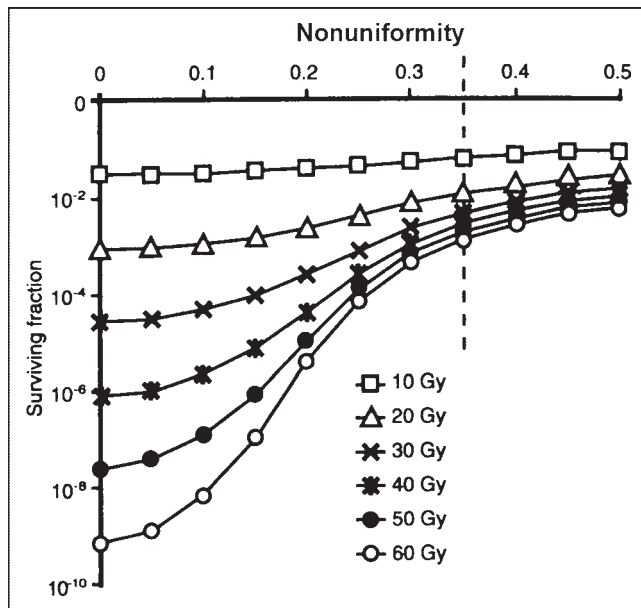


FIGURE 7. Therapeutic impact of nonuniform tumor-dose distribution. Surviving fraction plotted as function of nonuniformity for differing mean absorbed doses (11).

to be of interest. When such radionuclides are selectively accumulated in the targeted tissues (e.g., tumors), their decay should result in highly localized energy deposition in the targeted tumor cells and minimal irradiation of surrounding normal host tissues.

The investigation of the therapeutic potential of α -particle emitters has focused mainly on 4 radionuclides: ^{211}At , ^{212}Bi , ^{213}Bi , and ^{225}Ac (Table 2). In vitro studies have demonstrated that the decrease in mammalian cell survival after exposure to uniformly distributed α -particles from these radionuclides is monoexponential (14,15). However, as predicted theoretically and shown experimentally after the decay of ^{211}At -labeled 5-astato-2'-deoxyuridine (^{211}At -UdR), these curves develop a tail when the dose is nonuniform (Figs. 6A and 6B) (2,10). Such studies have also shown that the traversal of 1–4 α -particles through a mammalian cell nucleus will kill the cell (2,14,15). In comparison, the LET of negatrons emitted by the decay of energetic β -emitters is $\sim 0.2 \text{ keV}/\mu\text{m}$ and, thus, up to 20,000 β -particles must traverse a cell nucleus for its sterilization.

Investigators have also assessed the therapeutic potential of α -particle emitters in tumor-bearing animals (16–19). For example, Bloomer et al. (16) have reported a dose-related prolongation in median survival when mice bearing an intraperitoneal murine ovarian tumor are treated with ^{211}At -tellurium colloid administered directly into the peri-

TABLE 2
 α -Particle Emitters: Physical Properties

Radionuclide	E_{av}^* (MeV)	R_{av}^\dagger (μm)	Half-life
^{211}At	6.79	60	7.2 h
^{212}Bi	7.80	75	61 min
^{213}Bi	8.32	84	46 min
^{225}Ac	6.83	61	10 d

*Mean energy of α -particles emitted per disintegration (12).

† Mean range of α -particles calculated using second order polynomial regression fit (data from [13]): $R = 3.87E + 0.75E^2 - 0.45$; where R is the range (in micrometers) in unit density matter and E is the α -particle energy (MeV).

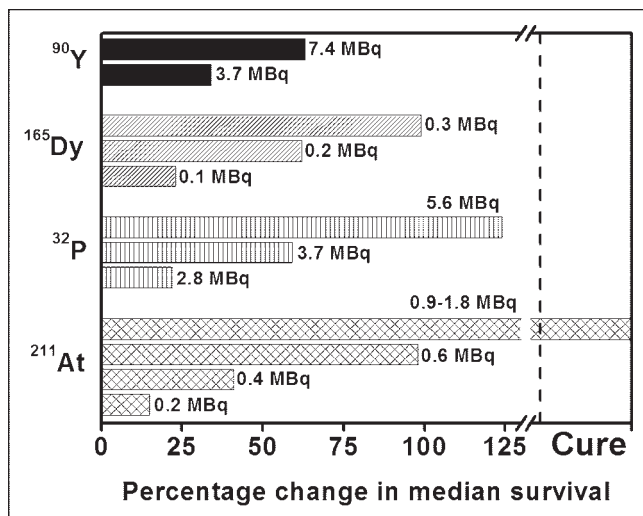


FIGURE 8. Percentage change in median survival of ovarian-cancer-bearing mice treated with α - or β -particle-emitting radiocolloids (16).

toneal cavity. Although this α -particle-emitting radiocolloid is curative without serious morbidity, β -particle-emitting radiocolloids (^{32}P , ^{165}Dy , ^{90}Y) are not (Fig. 8). In another set of *in vivo* studies examining the therapeutic efficacy of a ^{212}Bi -labeled monoclonal antibody, the radionuclide is found to be most effective when used with a carrier that entails target specificity (17). Finally, a report by McDevitt et al. (19) has demonstrated that ^{225}Ac -labeled internalizing antibodies are therapeutically effective in mice bearing solid prostate carcinoma or disseminated lymphoma.

β -Particle Emitters. Radionuclide-based tumor therapy has been performed mostly with β -particle emitters. Studies

have indicated that the exposure of cells *in vitro* to β -particles leads, in general, to survival curves with a distinct shoulder and a D_0 of several thousand decays (20,21). Despite rather low *in vitro* toxicity, these radionuclides continue to be pursued for targeted therapy. To a large extent, this is because of the availability and favorable characteristics of many energetic β -particle-emitting isotopes (Table 3). The long range (millimeters to centimeters) of the emitted electrons can lead to irradiation of all cells within the maximum range and path of the particle (i.e., cross-fire). As mentioned previously, the main advantage of cross-fire is that it negates the necessity of the radiotherapeutic agent being present within each of the targeted cells (i.e., it counteracts a certain degree of heterogeneity).

However, to deliver an effective therapeutic dose to the targeted tissue, the following conditions must be met: (a) the radiotherapeutic agent must concentrate within foci throughout the targeted tumor mass; (b) the distances between these hot foci must be equal to or less than twice the maximum range of the emitted energetic β -particles; and (c) the concentration of the radiotherapeutic agent within each hot focus must be sufficiently high to produce a cumulative cross-fire dose to the surrounding targeted cells of 10,000 cGy or more. Because dose is inversely proportional to square of the distance, the concentration of the therapeutic agent needed to deposit such cytotoxic doses increases markedly when the distance between the hot foci increases.

These predictions have been substantiated experimentally in various animal tumor therapy studies. For example, investigators have assessed the therapeutic efficacy of ^{131}I -labeled monoclonal antibodies in rodents bearing subcutaneous tumors. Although a substantial proportion of cells within a tumor mass show either reduced or no expression

TABLE 3
 β -Particle Emitters: Physical Properties

Radionuclide	Half-life	$E_{\beta^-(\text{min})}^*$ (keV)	$R_{\beta^-(\text{min})}^\dagger$ (mm)	$E_{\beta^-(\text{min})}/$ volume	$E_{\beta^-(\text{max})}^\ddagger$ (keV)	$R_{\beta^-(\text{max})}^\ddagger$ (mm)	$E_{\beta^-(\text{max})}/$ volume
^{33}P	25.4 d	77	0.09	2.0E5	249	0.63	1,902
^{177}Lu	6.7 d	47	0.04	1.4E6	497	1.8	174
^{67}Cu	61.9 h	51	0.05	7.8E5	575	2.1	119
^{131}I	8.0 d	69	0.08	2.6E5	606	2.3	95
^{186}Re	3.8 d	308	0.9	807	1,077	4.8	19
^{165}Dy	2.3 h	82	0.1	1.6E5	1,285	5.9	12
^{89}Sr	50.5 d	583	2.2	105	1,491	7.0	8.3
^{32}P	14.3 d	695	2.8	61	1,710	8.2	5.9
^{166}Ho	28.8 h	651	2.5	80	1,854	9.0	4.9
^{188}Re	17.0 h	528	1.9	147	2,120	10.4	3.6
^{90}Y	64.1 h	935	4.0	28	2,284	11.3	3.0

*Average minimum energy of least energetic β -particle emitted per disintegration (>1% intensity).

† Range (in micrometers) for electrons with $E = 0.02$ –100 keV calculated using Cole's equation (4): $R = 0.043(E + 0.367)^{1.77} - 0.007$; whereas range (in millimeters) for electrons with E -MeV calculated using second order fits (data from [22]): $R_{(0.1-0.5 \text{ MeV})} = 2.4E + 2.86E^2 - 0.14$, and $R_{(0.5-2.5 \text{ MeV})} = 5.3E + 0.0034E^2 - 0.93$.

‡ Maximum energy of β -particles emitted per disintegration.

TABLE 4
Auger-Electron Emitters: Physical Properties

Radionuclide	#*	Half-life	Total electron yield per decay		
			"Long"-range electrons (%)	"Short"-range electrons (%)	"Very short"-range electrons (%)
¹²⁵ I	20	60.5 d	20 (98%)	18 (86%)	8 (39%)
¹²³ I	11	13.3 h	11 (98%)	10 (89%)	5 (40%)
⁷⁷ Br	7	57 h	7 (100%)	6 (95%)	3 (51%)
¹¹¹ In	15	3 d	15 (98%)	14 (91%)	8 (53%)
^{193m} Pt	30	4.3 d	29 (97%)	28 (93%)	6 (21%)
^{195m} Pt	36	4 d	33 (92%)	33 (79%)	7 (19%)

Range:	<0.5 μm	<100 nm	<2 nm
LET†:	4–26	9–26	<18

*Average number of electrons emitted per decay.

†Fit of data from Cole (4).

of the targeted antigen and, therefore, are not targeted by the radioiodinated antibody. ¹³¹I-labeled antibodies that localize in high concentrations in tumors are therapeutically efficacious and can lead to total tumor eradication (23,24). Thus, even when ¹³¹I is not so uniformly distributed within a tumor, the decay of this radionuclide can lead to tumor sterilization as long as it is present in sufficiently high concentrations. Similar results have also been reported with radiopharmaceuticals labeled with other β-particle-emitting isotopes, in particular ⁹⁰Y (25–27) and ⁶⁷Cu (28). An important outcome of these findings has been the introduction of ¹³¹I- and ⁹⁰Y-labeled antibodies in the clinic.

Nonenergetic Particles

The toxicity to mammalian cells of radionuclides that decay by EC or IC has, for the most part, been established with ¹²⁵I. Dosimetric calculations with this and other Auger-electron-emitting radionuclides (Table 4) have shown that (a) multiple electrons are emitted per decaying atom; (b) the distances traversed by these electrons are mainly in the nanometer range; (c) the LET of the electrons is >20-fold higher than that observed along the tracks of energetic (>50 keV) β-particles; and (d) many of the emitted electrons dissipate their energy in the immediate vicinity of the decaying atom and deposit 10⁶ to 10⁹ rad/decay within a few-nanometer sphere around the decay site (7,8,29–32). From a radiobiologic prospective, the tridimensional organization of chromatin within the mammalian cell nucleus involves many structural level compactations (nucleosome, 30-nm chromatin fiber, chromonema fiber, etc.) with dimensions that are all within the range of these high-LET (4–26 keV/μm), low-energy (≤1.6 keV), short-range (≤150 nm) electrons. Therefore, the toxicity of Auger-electron-emitting radionuclides is expected to depend critically on close proximity of the decaying atom to DNA and to be quite high. These expectations have been substantiated by in

vitro studies showing that (a) the decay of Auger-electron emitters covalently bound to nuclear DNA leads to a monoexponential decrease in survival (8,33,34); (b) the curves may or may not exhibit a shoulder when the decaying atoms are not covalently bound to nuclear DNA (35–37); and (c) in general, intranuclear decay accumulation is highly toxic ($D_0 = \sim 100\text{--}500$ decays/cell), whereas decay within the cytoplasm or extracellularly produces no extraordinary lethal effects and yields survival curves that resemble those observed with X-rays (have a distinct shoulder) (38,39).

The extreme degree of cytotoxicity observed with DNA-incorporated Auger-electron emitters has been exploited in experimental radionuclide therapy. In most of these in vivo studies, the thymidine analog 5-iodo-2'-deoxyuridine (IUdR) has been used (40–42), and the

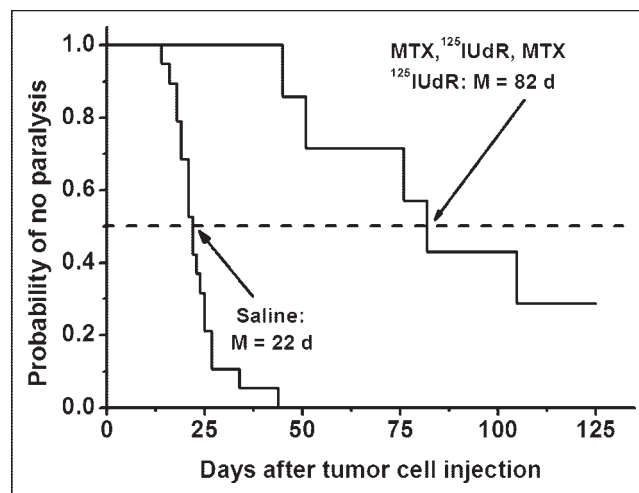


FIGURE 9. Induction of hind leg paralysis in rats by intrathecally growing human tumor cells after saline or methotrexate-¹²⁵I-UdR treatment.

results have shown excellent therapeutic efficacy. For example, the injection of ^{125}I -UdR into mice bearing an intraperitoneal ascites ovarian cancer has led to a 5-log reduction in tumor cell survival (40). Similar results have been obtained with ^{123}I -UdR (41). Therapeutic doses of ^{125}I -UdR injected intrathecally into rats with intrathecal tumors significantly delay the onset of paralysis, and the coadministration of methotrexate, an antimetabolite that enhances ^{125}I -UdR uptake by DNA-synthesizing cells, leads to a substantial enhancement in therapeutic efficacy as exemplified by a 5- to 6-log tumor cell kill and the curing of ~30% of the tumor-bearing rats (Fig. 9) (42).

CONCLUSION

A significant increase in our understanding of the dosimetry, radiobiologic effects, and therapeutic potential of various modes of radioactive decay has heightened the possibility of utilizing specifically labeled carriers in cancer therapy. Moreover, as a consequence of advances in genomics, the development of more precise targeting molecules is at hand. Further progress in the field of targeted radionuclide therapy will be made by the judicious design of radiolabeled molecules that match the physical and chemical characteristics of both the radionuclide and the carrier molecule with the clinical character of the tumor.

ACKNOWLEDGMENTS

Preparation of this article was supported by grants from the U.S. Department of Energy (DE-FG02-96ER62176) and the National Institutes of Health (5 R01 CA15523).

REFERENCES

- Steele GG, ed. *Basic Clinical Radiobiology*. 2nd ed. London, UK: Arnold; 1997:1-254.
- Walicka MA, Vaidyanathan G, Zalutsky MR, Adelstein SJ, Kassis AI. Survival and DNA damage in Chinese hamster V79 cells exposed to alpha particles emitted by DNA-incorporated astatine-211. *Radiat Res*. 1998;150:263-268.
- Goddu SM, Howell RW, Rao DV. Cellular dosimetry: absorbed fractions for monoenergetic electron and alpha particle sources and S-values for radionuclides uniformly distributed in different cell compartments. *J Nucl Med*. 1994;35:303-316.
- Cole A. Absorption of 20-eV to 50,000-eV electron beams in air and plastic. *Radiat Res*. 1969;38:7-33.
- Sastry KSR, Howell RW, Rao DV, et al. Dosimetry of Auger emitters: physical and phenomenological approaches. In: Baverstock KF, Charlton DE, eds. *DNA Damage by Auger Emitters*. London, UK: Taylor and Francis; 1988:27-38.
- Wright HA, Hamm RN, Turner JE, Howell RW, Rao DV, Sastry KSR. Calculations of physical and chemical reactions with DNA in aqueous solution from Auger cascades. *Radiat Prot Dosim*. 1990;31:59-62.
- Kassis AI, Adelstein SJ, Haydock C, Sastry KSR, McElvany KD, Welch MJ. Lethality of Auger electrons from the decay of bromine-77 in the DNA of mammalian cells. *Radiat Res*. 1982;90:362-373.
- Kassis AI, Sastry KSR, Adelstein SJ. Kinetics of uptake, retention, and radiotoxicity of ^{125}I UdR in mammalian cells: implications of localized energy deposition by Auger processes. *Radiat Res*. 1987;109:78-89.
- Barendswaard EC, O'Donoghue JA, Larson SM, et al. ^{131}I radioimmunotherapy and fractionated external beam radiotherapy: comparative effectiveness in a human tumor xenograft. *J Nucl Med*. 1999;40:1764-1768.
- Humm JL, Chin LM, Cobb L, Begent R. Microdosimetry in radioimmunotherapy. *Radiat Prot Dosim*. 1990;31:433-436.
- International Commission on Radiation Units and Measurements. Absorbed-dose specification in nuclear medicine (ICRU Report 67). *J ICRU*. 2002;2:29.
- Kocher DC. *Radioactive Decay Data Tables: A Handbook of Decay Data for Application to Radiation Dosimetry and Radiological Assessments*. Springfield, VA: National Technical Information Center, US Department of Energy; 1981: 1-221.
- International Commission on Radiation Units and Measurements. *Stopping Powers and Ranges for Protons and Alpha Particles*, Report 49. Bethesda, MD: International Commission on Radiation Units and Measurements; 1993: 256.
- Kassis AI, Harris CR, Adelstein SJ, Ruth TJ, Lambrecht R, Wolf AP. The *in vitro* radiobiology of astatine-211 decay. *Radiat Res*. 1986;105:27-36.
- Charlton DE, Kassis AI, Adelstein SJ. A comparison of experimental and calculated survival curves for V79 cells grown as monolayers or in suspension exposed to alpha irradiation from ^{212}Bi distributed in the growth medium. *Radiat Prot Dosim*. 1994;52:311-315.
- Bloomer WD, McLaughlin WH, Lambrecht RM, et al. ^{211}At radiocolloid therapy: further observations and comparison with radiocolloids of ^{32}P , ^{165}Dy , and ^{90}Y . *Int J Radiat Oncol Biol Phys*. 1984;10:341-348.
- Macklis RM, Kinsey BM, Kassis AI, et al. Radioimmunotherapy with alpha-particle-emitting immunoconjugates. *Science*. 1988;240:1024-1026.
- Zalutsky MR, McLendon RE, Garg PK, Archer GE, Schuster JM, Bigner DD. Radioimmunotherapy of neoplastic meningitis in rats using an alpha-particle-emitting immunoconjugate. *Cancer Res*. 1994;54:4719-4725.
- McDevitt MR, Ma D, Lai LT, et al. Tumor therapy with targeted atomic nanogenerators. *Science*. 2001;294:1537-1540.
- Chan PC, Lisco E, Lisco H, Adelstein SJ. The radiotoxicity of iodine-125 in mammalian cells. II. A comparative study on cell survival and cytogenetic responses to ^{125}I UdR, ^{131}I UdR, and $^3\text{HTdR}$. *Radiat Res*. 1976;67:332-343.
- Burki HJ, Koch C, Wolff S. Molecular suicide studies of ^{125}I and ^3H disintegration in the DNA of Chinese hamster cells. *Curr Top Radiat Res Q*. 1977;12: 408-425.
- International Commission on Radiation Units and Measurements. *Stopping Powers for Electrons and Positrons*, Report 37. Bethesda, MD: International Commission on Radiation Units and Measurements; 1984:1-271.
- Esteban JM, Schlom J, Mornex F, Colcher D. Radioimmunotherapy of athymic mice bearing human colon carcinomas with monoclonal antibody B72.3: histological and autoradiographic study of effects on tumors and normal organs. *Eur J Cancer Clin Oncol*. 1987;23:643-655.
- Buchsbaum D, Khazaeli MB, Liu T, et al. Fractionated radioimmunotherapy of human colon carcinoma xenografts with ^{131}I -labeled monoclonal antibody CC49. *Cancer Res*. 1995;55(suppl):5881s-5887s.
- Otte A, Mueller-Brand J, Dellas S, Nitzsche EU, Herrmann R, Maecke HR. Yttrium-90-labelled somatostatin-analogue for cancer treatment. *Lancet*. 1998; 351:417-418.
- Chinn PC, Leonard JE, Rosenberg J, Hanna N, Anderson DR. Preclinical evaluation of ^{90}Y -labeled anti-CD20 monoclonal antibody for treatment of non-Hodgkin's lymphoma. *Int J Oncol*. 1999;15:1017-1025.
- Axworthy DB, Reno JM, Hylarides MD, et al. Cure of human carcinoma xenografts by a single dose of pretargeted yttrium-90 with negligible toxicity. *Proc Natl Acad Sci USA*. 2000;97:1802-1807.
- DeNardo GL, Kukis DL, Shen S, et al. Efficacy and toxicity of ^{67}Cu -2IT-BAT-Lym-1 radioimmunoconjugate in mice implanted with human Burkitt's lymphoma (Raji). *Clin Cancer Res*. 1997;3:71-79.
- Kassis AI, Adelstein SJ, Haydock C, Sastry KSR. Radiotoxicity of ^{75}Se and ^{35}S : theory and application to a cellular model. *Radiat Res*. 1980;84:407-425.
- Kassis AI, Adelstein SJ, Haydock C, Sastry KSR. Thallium-201: an experimental and a theoretical radiobiological approach to dosimetry. *J Nucl Med*. 1983;24: 1164-1175.
- Charlton DE, Pomplun E, Booz J. Some consequences of the Auger effect: fluorescence yield, charge potential, and energy imparted. *Radiat Res*. 1987;111: 553-564.
- Kassis AI, Makrigiorgos GM, Adelstein SJ. Implications of radiobiological and dosimetric studies of DNA-incorporated ^{123}I : the use of the Auger effect as a biological probe at the nanometre level. *Radiat Prot Dosim*. 1990;31:333-338.
- Hofer KG, Hughes WL. Radiotoxicity of intranuclear tritium, ^{125}I iodine and ^{131}I iodine. *Radiat Res*. 1971;47:94-109.
- Chan PC, Lisco E, Lisco H, Adelstein SJ. Cell survival and cytogenetic responses to ^{125}I -UdR in cultured mammalian cells. *Curr Top Radiat Res Q*. 1977;12:426-435.
- Martin RF, Bradley TR, Hodgson GS. Cytotoxicity of an ^{125}I -labeled DNA-binding compound that induces double-stranded DNA breaks. *Cancer Res*. 1979; 39:3244-3247.

36. Bloomer WD, McLaughlin WH, Weichselbaum RR, et al. Iodine-125-labelled tamoxifen is differentially cytotoxic to cells containing oestrogen receptors. *Int J Radiat Biol.* 1980;38:197–202.
37. Walicka MA, Ding Y, Roy AM, Harapanhalli RS, Adelstein SJ, Kassis AI. Cytotoxicity of [¹²⁵I]iodoHoechst 33342: contribution of scavengeable effects. *Int J Radiat Biol.* 1999;75:1579–1587.
38. Hofer KG, Harris CR, Smith JM. Radiotoxicity of intracellular ⁶⁷Ga, ¹²⁵I and ³H: nuclear versus cytoplasmic radiation effects in murine L1210 leukaemia. *Int J Radiat Biol.* 1975;28:225–241.
39. Kassis AI, Fayad F, Kinsey BM, Sastry KSR, Taube RA, Adelstein SJ. Radiotoxicity of ¹²⁵I in mammalian cells. *Radiat Res.* 1987;111:305–318.
40. Bloomer WD, Adelstein SJ. 5-¹²⁵I-iododeoxyuridine as prototype for radionuclide therapy with Auger emitters. *Nature.* 1977;265:620–621.
41. Baranowska-Kortylewicz J, Makrigiorgos GM, Van den Abbeele AD, Berman RM, Adelstein SJ, Kassis AI. 5-[¹²³I]iodo-2'-deoxyuridine in the radiotherapy of an early ascites tumor model. *Int J Radiat Oncol Biol Phys.* 1991;21:1541–1551.
42. Kassis AI, Dahman BA, Adelstein SJ. In vivo therapy of neoplastic meningitis with methotrexate and 5-[¹²⁵I]iodo-2'-deoxyuridine. *Acta Oncol.* 2000;39:731–737.





The Journal of
NUCLEAR MEDICINE

Radiobiologic Principles in Radionuclide Therapy

Amin I. Kassis and S. James Adelstein

J Nucl Med. 2005;46:4S-12S.

This article and updated information are available at:
http://jnm.snmjournals.org/content/46/1_suppl/4S

Information about reproducing figures, tables, or other portions of this article can be found online at:
<http://jnm.snmjournals.org/site/misc/permission.xhtml>

Information about subscriptions to JNM can be found at:
<http://jnm.snmjournals.org/site/subscriptions/online.xhtml>

The Journal of Nuclear Medicine is published monthly.
SNMMI | Society of Nuclear Medicine and Molecular Imaging
1850 Samuel Morse Drive, Reston, VA 20190.
(Print ISSN: 0161-5505, Online ISSN: 2159-662X)

© Copyright 2005 SNMMI; all rights reserved.